

Pearl drops

J. BICO¹, C. MARZOLIN² and D. QUÉRÉ¹

¹ *Laboratoire de Physique de la Matière Condensée
URA 792 du CNRS, Collège de France
75231 Paris Cedex 05, France*

² *Saint-Gobain Recherche - 39 quai Lucien-Lefranc
93303 Aubervilliers Cedex, France*

(received 4 January 1999; accepted in final form 6 May 1999)

PACS. 68.10-m – Fluid surfaces and fluid-fluid interfaces.

PACS. 68.15+e – Liquid thin films.

Abstract. – If deposited on a hydrophobic rough substrate, a small drop of water can look like a pearl, with a contact angle close to 180°. We examine the conditions for observing such a phenomenon and show practical achievements where the contact angle can be predicted and thus quantitatively tuned by the design of the surface microstructure.

Presentation. – The contact angle of a drop on a solid is ideally (for a flat homogeneous solid) given by the classical *Young's equation*:

$$\cos \theta = \frac{\gamma_{SV} - \gamma_{SL}}{\gamma}, \quad (1)$$

where γ_{SV} , γ_{SL} and γ are the different surface tensions (solid/vapor, solid/liquid and liquid/vapor) involved in the system.

Here we describe how the contact angle can be modified by the surface texture and focus on the limit of practical interest where very large contact angles can be obtained [1, 2]. Such surfaces were recently achieved by the Kao group [3, 4]: a water drop put on fractal hydrophobic surfaces was found to have contact angles of order 170°. On some leaves (for example lotus or lily-water), water drops are also found to be nearly spherical (contact angles of order 160°) [5]. Here, we exhibit the relevant parameters for obtaining such angles and present new data obtained with model surfaces.

Simple models. – Wenzel proposed the first approach to characterize the influence of the surface roughness on the wettability of a solid [6]. The contact angle θ^* on a rough surface can be evaluated by considering a little displacement dx of the contact line parallel to the surface (fig. 1).

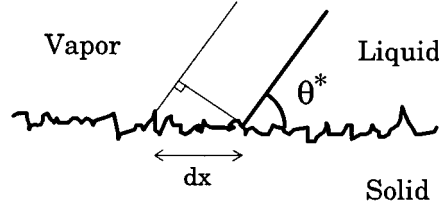


Fig. 1. – Infinitesimal spreading of a liquid wedge on a rough surface.

Then, the surface energies (written per unit length of the contact line) are modified of a quantity dF given by:

$$dF = r(\gamma_{SL} - \gamma_{SV})dx + \gamma dx \cos \theta^*, \tag{2}$$

where r is the solid roughness, defined as the ratio between the real surface and the projected one. The equilibrium is given by the minimum of F , from which we get *Wenzel's equation*:

$$\cos \theta^* = r \cos \theta, \tag{3}$$

where θ is Young's angle, given in eq. (1). This simple model shows that the effect of surface roughness is to amplify the wetting. Since we always have $r > 1$, the wetting gets better in hydrophilic situations ($\theta^* < \theta$ for $\theta < \pi/2$) and worse in hydrophobic ones ($\theta^* > \theta$ for $\theta > \pi/2$).

For $\theta > \pi/2$, the surface energy of the dry solid is lower than the surface energy of the wet solid ($\gamma_{SV} < \gamma_{SL}$) and thus it is expected that the contact line does not follow the accidents of the solid surface, as supposed for establishing eq. (3). In this case, the drop is rather laid on a composite surface, patchwork of solid and air, as shown directly by Barthlott and Neinhuis [7] who could take photomicrographs of drops on a hydrophobic leaf.

We can evaluate how the existence of these air pockets modifies the contact angle. The simplest way to treat this problem is to consider a crenellated surface (or equivalently full of holes), as in fig. 2a.

Then, displacing the contact line of a quantity dx parallel to the surface implies a change in surface energy dF equal to:

$$dF = \phi_s(\gamma_{SL} - \gamma_{SV})dx + (1 - \phi_s)\gamma dx + \gamma dx \cos \theta^*, \tag{4}$$

where ϕ_s is the solid fraction of the surface. The thin lines in fig. 2a are the liquid/vapor interfaces (occupying a surface fraction $1 - \phi_s$) below the liquid drop. Since the drop is much

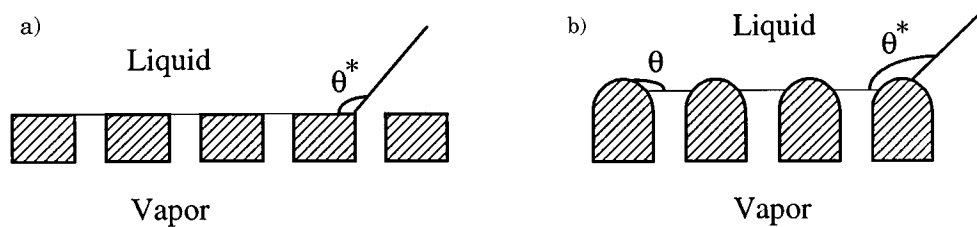


Fig. 2. – Liquid deposited on a model surface with holes (a) crenellated surface; b) hemispherical bumps): for contact angles larger than $\pi/2$, air is trapped below the liquid, inducing a composite interface between the solid and the drop.

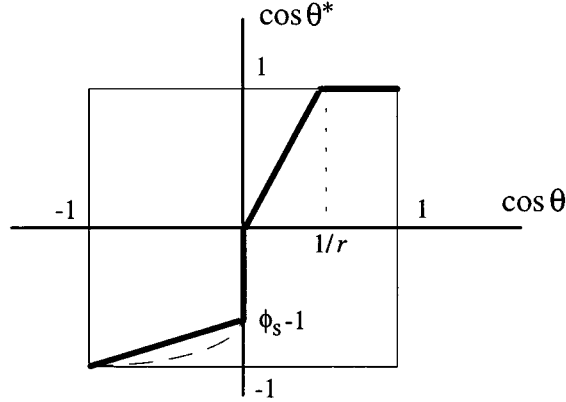


Fig. 3. – Cosine of the effective contact angle θ^* of a drop on a rough model surface as a function of the cosine of the Young contact angle θ . r is the solid roughness and ϕ_s is the surface solid fraction. On the hydrophobic side ($\cos \theta < 0$), the full line is eq. (5) and the dotted one is eq. (6).

larger than the air pockets and because of the condition of a constant Laplace pressure inside the drop, these interfaces can be drawn straight. Furthermore, all these interfaces are pinned on the corners of the crenellations, the condition of pinning of a contact line on such corners being precisely a contact angle larger than $\pi/2$ [8].

At equilibrium, F is minimum and we get (using Young's equation):

$$\cos \theta^* = -1 + \phi_s(\cos \theta + 1). \quad (5)$$

Equation (5) is a particular form of the Cassie-Baxter law which gives the contact angle for a drop deposited on a composite surface: the cosine of this angle is the average of the cosines of the different contact angles, weighed by the respective surface fractions of the heterogeneities [9]. It is plotted in full line in fig. 3 for $\theta > \pi/2$, while keeping the Wenzel equation on the hydrophilic side ($\theta < \pi/2$).

Of course, taking crenellations for modelling the surface is an approximation. On a given rough surface, the fraction ϕ_s itself is a function of the contact angle θ . Let us suppose for example that the solid fraction is not flat but ends with hemispherical bumps (fig. 2b). Then, the liquid/vapor interfaces (still in thin line) are located where the Young condition is fulfilled: the surface of solid in contact with the liquid is all the larger since the contact angle is low. Finally, we can calculate the way ϕ_s depends on θ and the effective contact angle θ^* of a drop, via equation (5). Elementary trigonometry gives

$$\cos \theta^* = -1 + \phi_B(\cos \theta + 1)^2, \quad (6)$$

where ϕ_B is the ratio of the surfaces of the spike bases over the total solid surface. Equation (6) is the parabolic dotted line in fig. 3 and turns out to have the same qualitative features as eq. (5). In both cases, the contact angle has a discontinuity when q becomes smaller than $\pi/2$, a major difference with Wenzel's equation. As soon as the contact angle is above this value, air is trapped below the drop which basically modifies the wetting. The limit of a surface which would be one single hole ($\phi_s = \phi_B = 0$) is of course $\theta = \pi$: a static drop in the air is spherical. Another difference with Wenzel's law is the fact that a π -angle is only asymptotic, which is physically reasonable.

These results can be compared with the data of the Kao group [4], which are displayed in fig. 4 for different solid roughnesses (increasing from left to right).

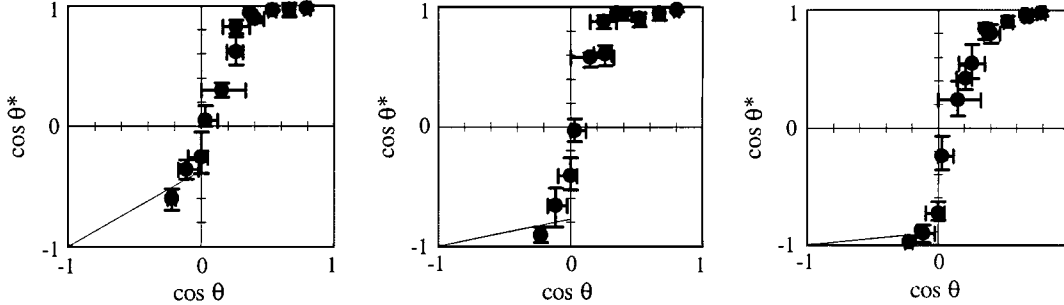


Fig. 4. – Experimental results of the Kao group (from [4]). The cosine of the effective contact angle θ^* of a water drop was measured as a function of the cosine of the Young angle θ (determined on a flat surface of the same material), for different solid roughnesses (increasing from left to right). The thin straight line is eq. (5) with ϕ_s as an adjustable parameter.

The main features of fig. 3 can be qualitatively observed in these data. In particular, there is a clear dissymmetry between the hydrophilic and hydrophobic sides. For $\cos \theta > 0$, the data can be described by a linear interpolation (Wenzel’s law), while a contact angle discontinuity is indeed observed close to $\cos \theta = 0$. The latter effect is all the more marked since the roughness is high. If treated as an adjustable parameter, a solid fraction ϕ_s can be deduced (thin lines in fig. 4): it is logically found to be a decreasing function of the solid roughness.

Since the values of the actual fraction of solid in contact with the liquid are unknown, we cannot get more than a qualitative agreement. To go further, we achieved surfaces with a controlled design of the roughness. We chose to build crenellated solids, because of the large difference in morphology with the fractal surfaces of the Kao group. Besides, it allowed us to compare directly the data with eq. (5).

Surfaces with a controlled design. – The reference surface is a silicon wafer made hydrophobic by grafting a self-assembled monolayer of fluorosilane ($\text{F}(\text{CF}_2)_{10}(\text{CH}_2)_2\text{SiCl}_3$). Contact angles against water were measured with a goniometer with a precision of order 1° . The advancing and receding contact angles were found to be $\theta_a = 118^\circ$ and $\theta_r = 100^\circ$; this hysteresis is quite small and the reference surface can be considered as close to be ideal.

The microstructures were created by molding a sol-gel of tetramethylorthosilicate between a bare silicon wafer and an elastomeric mold designed by replicating a pattern in photoresist.

TABLE I. – Measurements of the solid surface fraction ϕ_s , the advancing and receding contact angles θ_a and θ_r for the different surfaces pictured in fig. 5. For small ϕ_s , a large increase of the contact angle is observed if compared with a flat surface of same hydrophobicity ($\phi_s = 1$). The measured contact angles θ_a are compared with the value θ^* predicted by eq. (5).

Pattern	ϕ_s	θ_a	θ_r	θ^*
Plane	1	118	100	
Holes	0.64	138	75	131
Stripes	0.25	165 (\perp)	132	151
	0.25	143 ($//$)	125	151
Spikes	0.05	170	155	167

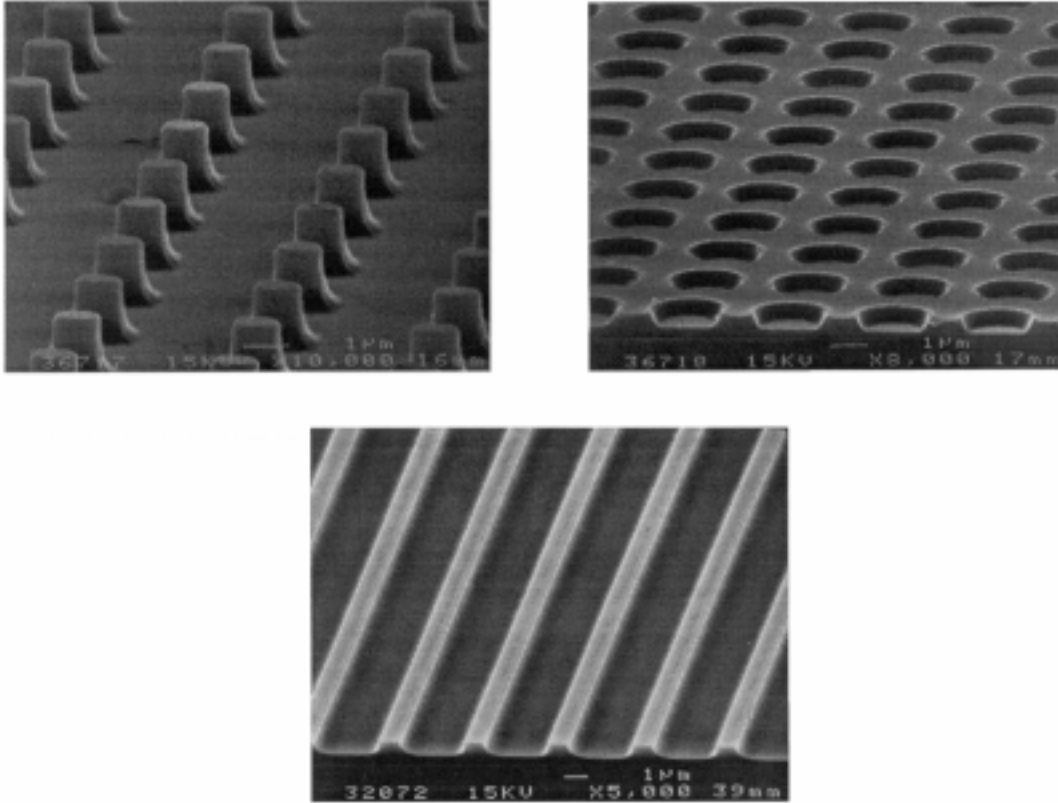


Fig. 5. – SEM images of microstructured hydrophobic surfaces designed for quantifying the influence of the surface pattern on the contact angle. The three different surfaces (spikes, shallow cavities and stripes) are crenellated on a micrometer scale.

After gellation, the silica structures were consolidated at 1100 °C for 2 h and rendered hydrophobic as described for the reference surface. Technical details are given in [10]. Three different types of crenellations were achieved: shallow cavities, stripes and for the first time spikes, as shown in fig. 5. All the defects are in the micrometer range.

The contact angles with water were finally measured on these surfaces and compared with the values θ^* deduced from eq. (5) (taking for θ the advancing contact angle on a plane of same hydrophobicity). It must be emphasized that the solid fraction ϕ_s is no longer an adjustable parameter, but can be precisely measured (precision of less than 5%) since it is the ratio of the upper surface of the crenellations over the total surface of the sample. Thus, it varies largely with the patterns (from 5% to 64%). All the results are displayed in table I.

For the two isotropic surfaces (holes and spikes), the advancing contact angle is found to be in very close agreement with eq. (5). It is outstandingly large for the spike structure, on which a water drop is indeed nearly spherical as shown in fig. 6. Note that the silicon surface remains reflective, because the periodic pattern only induces diffraction and no diffuse scattering of light.

Since the receding angle is also quite large on this surface, it really behaves as repellent for water: it was nearly impossible to maintain a drop to take the picture reproduced in fig. 6. The hole surface does not have this property, because of a much higher solid fraction which

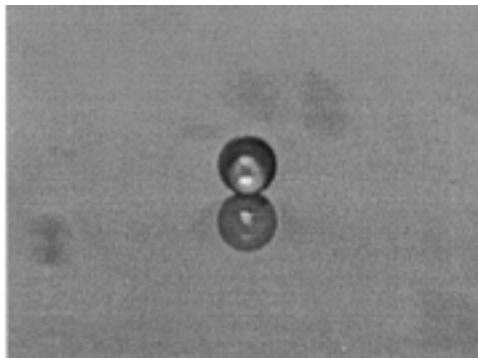


Fig. 6. – Water drop on a hydrophobic surface decorated with spikes (see the microscopic pattern in fig. 5). The drop has a radius of $100\ \mu\text{m}$.

makes the contact angle smaller. Furthermore, the receding angle is very small (with a large hysteresis of about 60°), which can be understood by the shallowness of the cavities which are able to retain water at the retraction. Using the Cassie-Baxter equation, the latter fact can be quantitatively confirmed: an average of the cosines of angles on solid and on *water* (0° contact angle), with as respective weights ϕ_s and $1 - \phi_s$, gives a receding contact angle of 75° , as observed.

The case of the stripes is slightly different because it introduces some anisotropy in wetting. Contact angles are different if measured parallelly or perpendicularly to the stripes, as reported in table I. There, the value deduced from eq. (5) is just indicative but appears to be between the two experimental values. The hysteresis is also found to depend on the direction of wetting.

Conclusion. – We have shown that the main parameter that determines the contact angle of a drop on a hydrophobic rough surface is the *fraction of solid* ϕ_s actually in contact with the liquid (eqs. (5) and (6)), and not the surface roughness itself as sometimes invoked for explaining the extreme hydrophobicity of very rough surfaces. Thus, it is not necessary to deal with fractal surfaces to get water-repellent surfaces: a flat surface decorated with spikes was shown to be highly hydrophobic, in spite of a low roughness ($r = 1.3$). This surface behaves like a *fakir carpet* for the drop, which is in contact only with the top of the spikes: since it mainly sits on air, the drop is nearly spherical.

Such surfaces are promising for both practical applications (rain-repellent coatings) and fundamental studies: in particular, we are currently studying the way a drop can roll on such a surface (instead of sliding) and bounce if thrown on it. But even the static problem of the contact angle of a pearl drop still raises interesting questions. For example, the resistance of the fakir carpet against the pressure due to the drop is finite. This limit can be easily computed by balancing the capillary force acting on one spike with the weight supported by this spike. When pressing on a drop, we indeed observe a change in the contact angle, which sharply decreases from 170° to $130^\circ (\pm 5^\circ)$. This effect can be interpreted as an impalement of the drop on the spikes, which implies a transition from eq. (5) to eq. (3): Wenzel's law indeed yields $\theta^* = 128^\circ$ for $r = 1.3$ and $\theta = 118^\circ$). Related questions are the search for the minimum solid fraction and defect size to get such a pearl drop, and as a consequence the possibility to achieve transparent repellent surfaces. In each case, the surface must have the ability to trap air. Here, this condition was ensured by considering solids with sharp edges. On more regular surfaces, a transition between the air trapping regime and the Wenzel one is

also expected when decreasing the maximum slope of the solid surface, as shown by Johnson and Dettre [1,2]. Thus, it would be worth building other surface designs, which could lead to a better understanding of the way the solid fraction adapts on an arbitrary rough surface (as the Kao one).

It is a pleasure to thank H. ARRIBART, V. COUSTET, L. DELATTRE, P. G. DE GENNES and D. RICHARD for numerous discussions and encouragement.

REFERENCES

- [1] JOHNSON R. E. and DETTRE R. H., in *Contact Angle, in Wettability and Adhesion, Adv. Chem. Ser.*, **43** (1964) 112.
- [2] DETTRE R. H. and JOHNSON R. E., in *Contact angle, in Wettability and Adhesion, Adv. Chem. Ser.* **43** (1964) 136.
- [3] ONDA T., SHIBUICHI S., SATOH N. and TSUJII K., *Langmuir*, **12** (1996) 2125.
- [4] SHIBUICHI S., ONDA T., SATOH N. and TSUJII K. J., *Phys. Chem.*, **100** (1996) 19512.
- [5] NEINHUIS C. and BARTHLOTT W., *Ann. Bot.*, **79** (1997) 667.
- [6] WENZEL R. N., *Ind. Eng. Chem.*, **28** (1936) 988; *J. Phys. Colloid Chem.*, **53** (1949) 1466.
- [7] BARTHLOTT W. and NEINHUIS C., *Planta*, **202** (1997) 1.
- [8] OLIVER J. F., HUH C. and MASON S. G., *J. Colloid Interface Sci.*, **59** (1977) 568.
- [9] CASSIE A. B. D. and BAXTER S., *Trans. Faraday Soc.*, **40** (1944) 546.
- [10] MARZOLIN C., SMITH S. P., PRENTISS M. and WHITESIDES G. M., *Adv. Mater.*, **10** (1998) 571.